

Testing the Copernican principle by constraining spatial homogeneity

Wessel Valkenburg,^{1,2} Valerio Marra,² and Chris Clarkson³

¹*Instituut-Lorentz for Theoretical Physics, Universiteit Leiden
Postbus 9506, 2333 CA Leiden, The Netherlands*

²*Institut für Theoretische Physik, Universität Heidelberg, Philosophenweg 16, 69120 Heidelberg, Germany*

³*Astrophysics, Cosmology and Gravity Centre, and Department of Mathematics and Applied Mathematics,
University of Cape Town, Rondebosch 7701, South Africa*

We present a new program for placing constraints on radial inhomogeneity in a dark-energy dominated universe. For the first time, we quantify restrictions on violations of the Copernican principle without neglecting dark energy. This is important because any violation of this principle would interfere with our interpretation of any dark-energy evolution. In particular, we find that current observations place reasonably tight constraints on possible late-time violations of the Copernican principle: the Figure of Merit in the parameter space of amplitude and scale of a spherical inhomogeneity around the observer has to be increased by a factor of 3 so as to confirm the Copernican principle. Then, by marginalising over possible radial inhomogeneity we provide the first constraints on the cosmological constant which are free of the homogeneity prior prevalent in cosmological modelling.

PACS numbers: 98.80.Es, 95.36.+x, 98.65.Dx

Keywords: Observational cosmology, dark energy, large-scale structure of the Universe, Copernican principle

Introduction The Copernican principle states that humans are not privileged observers of the universe and provides our philosophical basis for assuming that on the largest scales the universe is spatially homogeneous. While it is one of the foundational aspects of modern cosmology, this assumption remains untested outside of the standard paradigm. Though it may seem pedantic to test something so obvious, the standard paradigm itself is built on shaky foundations, relying on an unexplained, gravitationally repulsive, dark-energy component for observations to fit the model. The implications of this cannot be overstated. Assuming that the laws of physics do apply equally everywhere in the universe, the only non-copernican configuration possible is one in which we live in a place that originates from special initial conditions. The implications for our observations today would be an expansion rate that is sourced by different energy components (matter, curvature, etc.) in different directions and at different distances. As current observations of the expansion rate of the universe suggest isotropy around us, any model that tries to explain part of the expansion history as a result of spatial variations inevitably places the observer near the centre of a spherically symmetric matter distribution. Because we can observe changes in the expansion of the universe as a function of redshift only, it remains hard to disentangle temporal evolution from possible spatial variations spherically around us. Indeed, there has even been active debate on models whereby (part of the) dark energy is replaced by radial inhomogeneity about us, in violation of the Copernican principle. While this seems highly unlikely and challenging to make work (see [1, 2] for reviews), it highlights how intertwined are attempts to detect any evolution of dark energy to the Copernican principle.

To rule out spherically symmetric models, consistency

tests have been proposed (see [2] for a review), but all suffer as they lack at present a quantifiable measure of deviations from homogeneity. Attempts have been made to measure the homogeneity of the universe, albeit ignoring possible violation of the copernican principle [3, 4]. We offer here a new approach, by directly constraining any radial change in the density, Hubble rate and curvature assuming the Copernican principle is false and that dark energy exists. We model the universe spherically symmetric, containing both matter and dark energy in the form of a cosmological constant. We provide marginalised constraints on the amplitude and scale of any spatial inhomogeneity, over- and under-dense, using all relevant available observational data.

We quantify the deviation from Copernicanism by comparing the constraints we find on the spherical inhomogeneity to the theoretical constraints on the existence of the same inhomogeneity in a Copernican universe. If the universe is Copernican, the temperature fluctuations observed in the CMB come from the same distribution as do matter perturbations around us. Observing the CMB, one can calculate the probability of having a spherical inhomogeneity of certain dimensions around us. The ratio of allowed volumes in parameter space, on the one hand constrained by observations on the lightcone and on the other hand by the distribution of the distant CMB density fluctuations, gives a measure of how far we are from establishing the Copernican principle observationally.

Finally, by marginalising over the inhomogeneity parameters, we provide constraints on Λ which are independent of the homogeneity assumption and any reliance on the Copernican principle, thus being the most robust to date.

The model We model radial inhomogeneity assuming a spherically symmetric Lemaître-Tolman-Bondi so-

lution including a cosmological constant Λ (ALTB, see e.g. [5–7]). The metric is given by ($c = 1$)

$$ds^2 = -dt^2 + \frac{a_{\parallel}^2(t, r)}{1 - k(r)r^2} dr^2 + a_{\perp}^2(t, r)r^2 d\Omega^2, \quad (1)$$

where the radial (a_{\parallel}) and angular (a_{\perp}) scale factors are related by $a_{\parallel} = (a_{\perp}r)'$. A prime denotes partial derivation with respect to the coordinate radius r . The curvature $k = k(r)$ is not constant but is instead a free function. The FLRW limit is $k \rightarrow \text{const.}$, and $a_{\perp} = a_{\parallel}$. The two scale factors define two Hubble rates:

$$H_{\perp} = H_{\perp}(t, r) \equiv \frac{\dot{a}_{\perp}}{a_{\perp}}, \quad H_{\parallel} = H_{\parallel}(t, r) \equiv \frac{\dot{a}_{\parallel}}{a_{\parallel}}. \quad (2)$$

The analogue of the Friedmann equation in this space-time is then given by $H_{\perp}^2 = M/a_{\perp}^3 - k/a_{\perp}^2 + \Lambda/3$, where $M = M(r)$ is another free function of r related to the locally measured matter density $8\pi G \rho_m(t, r) = (Mr^3)' / a_{\parallel} a_{\perp}^2 r^2$, which obeys the conservation equation $\dot{\rho}_m + (2H_{\perp} + H_{\parallel})\rho_m = 0$. We introduce dimensionless density parameters for the CDM and curvature, by analogy with the FLRW models:

$$\Omega_m(r) = \frac{M}{H_{\perp 0}^2}, \quad \Omega_k(r) = -\frac{k}{H_{\perp 0}^2}, \quad \Omega_{\Lambda}(r) = \frac{\Lambda}{3H_{\perp 0}^2}, \quad (3)$$

so that $\Omega_m(r) + \Omega_k(r) + \Omega_{\Lambda}(r) = 1$. Note that in the previous equation the gauge fixing $a_{\perp}(t_0, r) = 1$ has been used. Moreover, Ω_{Λ} depends on r because the present-day expansion rate $H_{\perp 0}$ is inhomogeneous. Using (3) the Friedmann equation takes on its familiar form:

$$\frac{H_{\perp}^2}{H_{\perp 0}^2} = \Omega_m a_{\perp}^{-3} + \Omega_k a_{\perp}^{-2} + \Omega_{\Lambda}. \quad (4)$$

Integrating the Friedmann equation from the time of the big bang $t_{\text{bb}}(r)$ to some later time t yields the age of the universe at a given (t, r) :

$$t - t_{\text{bb}} = \frac{1}{H_{\perp 0}(r)} \int_0^{a_{\perp}(t, r)} \frac{dx}{\sqrt{\Omega_m(r)x^{-1} + \Omega_k(r) + \Omega_{\Lambda}(r)x^2}}. \quad (5)$$

Hence there is a relation between the functions t_{bb} , Ω_k and Ω_m . Therefore the ALTb model is specified by two free functional degrees of freedom, and we will use $\Omega_k(r)$ and $t_{\text{bb}}(r)$. By demanding a homogeneous age of the universe we fix the bang function to zero, $t_{\text{bb}}(r) = 0$. This ensures the absence of decaying modes in the matter density [8, 9], in agreement with the standard inflationary scenario.

We parametrize the only left freedom with the curvature function with the monotonic profile

$$k_{\alpha}(r) = k_b + (k_c - k_b) P_3\left(\frac{r}{r_b}, \alpha\right), \quad (6)$$

where r_b is the comoving radius of the spherical inhomogeneity and

$$P_n(x, \alpha) = \begin{cases} 1 & \text{for } 0 \leq x < \alpha \\ 1 - e^{-\frac{1-\alpha}{x-\alpha}(1-\frac{x-\alpha}{1-\alpha})^n} & \text{for } \alpha \leq x < 1 \\ 0 & \text{for } x \geq 1 \end{cases}.$$

Now $k_{\alpha}(r)$ is C^n everywhere. We choose $n = 3$, such that the metric is C^2 and the Riemann curvature is C^0 . For $r \geq r_b$ the curvature profile equals k_b such that there the metric describes exactly the Λ CDM model. The central over- or under-density, determined by curvature k_c , is automatically compensated by a surrounding under- or over-dense shell. The smoothness of the transition from k_c to k_b is parameterized by α . Hence r_b , k_c , k_b and α are free parameters.

Finally, on the past light cone of a central observer, $t(z)$ and $r(z)$ are determined by the differential equations for radial null geodesics,

$$\frac{dt}{dz} = -\frac{1}{(1+z)H_{\parallel}}, \quad \frac{dr}{dz} = \frac{\sqrt{1 - kr^2}}{(1+z)a_{\parallel}H_{\parallel}}, \quad (7)$$

where H_{\parallel} and a_{\parallel} are evaluated on the light cone. The area (d_A) and luminosity (d_L) distances are given by

$$d_A(z) = a_{\perp}(t(z), r(z)) r(z), \quad d_L = (1+z)^2 d_A. \quad (8)$$

Data & Observables

H₀: We compare a local average of the Hubble rate [10],

$$H_0 = \frac{1}{z_{\text{max}} - z_{\text{min}}} \int_{z_{\text{min}}}^{z_{\text{max}}} H_{\perp}(r(z), t(z)) dz, \quad (9)$$

with the value measured by [11] of $H_{\text{Freedman}} = 72 \pm 8$ km s⁻¹ Mpc⁻¹. We choose $z_{\text{min}} = 0.005$ and $z_{\text{max}} = 0.1$.

Supernovae Ia: We use the SNLS3 catalogue [12], which consists of 472 type Ia supernovae in the redshift range $z = 0.01 - 1.39$.

CMB: We fit the CMB according to the method presented in [13, 14], in which an effective FLRW metric is used to account for the different area distance to the surface of last scattering as compared to the homogeneous background model. This method ignores isocurvature modes (consistent with the choice of a homogeneous big bang), assumes a standard number of relativistic degrees of freedom and a standard power spectrum, all of which would change the constraints [2]. We fit our model to the WMAP 7-year data release [15].

BAO: The sound horizon during the drag epoch is imprinted in the galaxy correlation function. In an inhomogeneous model this is an ellipsoid with proper scales, when viewed from the centre

$$L_{\perp}(z) = d_s \frac{a_{\perp}(z)}{a_{\perp}(t_d, r(z))} = d_A(z) \theta_s(z), \quad (10)$$

$$L_{\parallel}(z) = d_s \frac{a_{\parallel}(z)}{a_{\parallel}(t_d, r(z))} = \frac{z_s(z)}{(1+z)H_{\parallel}(z)}, \quad (11)$$

where θ_s is the angle that the acoustic scale subtends on the sky, and z_s is the redshift interval corresponding to the acoustic scale in the radial direction. The sound horizon d_s is calculated assuming a homogeneous early universe. We use observations from SDSS, 6DFGS and WiggleZ [16–18], as compiled in [19].

Compton y -distortion: Off-centre observers see a large dipole in the CMB in an inhomogeneous universe. CMB photons are scattered from inside our past light-cone into our line-of-sight by off-centre reionized structures which act as mirrors. The spectrum observed by the central observer is, therefore, a mixture of black-body spectra with different temperatures, producing a distorted black-body spectrum. In the single-scattering and linear approximations, and when the temperature anisotropy is dominated by the induced dipole β , the y -distortion can be written as [13]:

$$y = \frac{7}{10} \int_0^{r_{\text{re}}} dr \frac{d\tau}{dr} \beta(r)^2, \quad (12)$$

where r is the comoving distance down the light cone and r_{re} marks the reionization epoch. The time dependence of the optical depth is given by $d\tau/dt = \sigma_T n_e(t) = \sigma_T f_b (1 - Y_{\text{He}}/2) \rho_m(t)/m_p$, where σ_T is the Thomson cross section, $f_b \equiv \rho_b/\rho_m$ is the baryon fraction, Y_{He} is the helium mass fraction and m_p is the proton mass. The dipole β is found by integrating the geodesic equations (7) in the negative and positive r -directions starting from an observer at $\{t(z), r(z)\}$ back to the surface of last scattering. The difference in redshift between the two directions is then approximately translated into the dipole observed by the scatter: $\beta = (z_+ - z_-)/(2 + z_+ + z_-)$. The 2σ upper limit from the COBE satellite [20] is $y < 1.5 \times 10^{-5}$. **kSZ:** The dipole β affects the observed CMB also through the kSZ effect [21]: hot electrons inside an overdensity distort the CMB spectrum through inverse Compton scattering, in which low energy CMB photons receive energy boosts during collisions with the high-energy electrons. We will focus here on the so-called “linear kSZ effect” [22], in which the effect due to all free electrons in the reionized universe is taken into account. Using the Limber approximation, the kSZ power at multipole ℓ is given by [23]

$$C_\ell^{\text{kSZ}} \simeq \frac{16\pi^2}{(2\ell + 1)^3} \int_0^{r_{\text{re}}} dr r \left[\beta(r) \frac{d\tau}{dr} \right]^2 \Delta_m^2(\hat{k}(r), r), \quad (13)$$

where $\Delta_m^2(k, z) = \frac{k^3}{2\pi^2} P_m(k, z)$ is the dimensionless power spectrum of the background model and the function $\hat{k}(r) \equiv \hat{k}(k(r), z(r))$ is necessary to “isotropize” the angular and radial wave numbers which in an inhomogeneous universe evolve differently: $\hat{k}(\bar{k}, z) = \bar{k}[(1 + \bar{z})a_\perp(\bar{t}, r(z))^{2/3} a_\parallel(\bar{t}, r(z))^{1/3}] / [(1 + z)a_\perp(z)^{2/3} a_\parallel(z)^{1/3}]$. We constrain inhomogeneous models using a top hat prior $0 < l(l + 1) [C_{\ell=3000}^{\text{TT}} + C_{\ell=3000}^{\text{kSZ}}] < 59 \mu\text{K}^2$, based on the results from SPT [24].

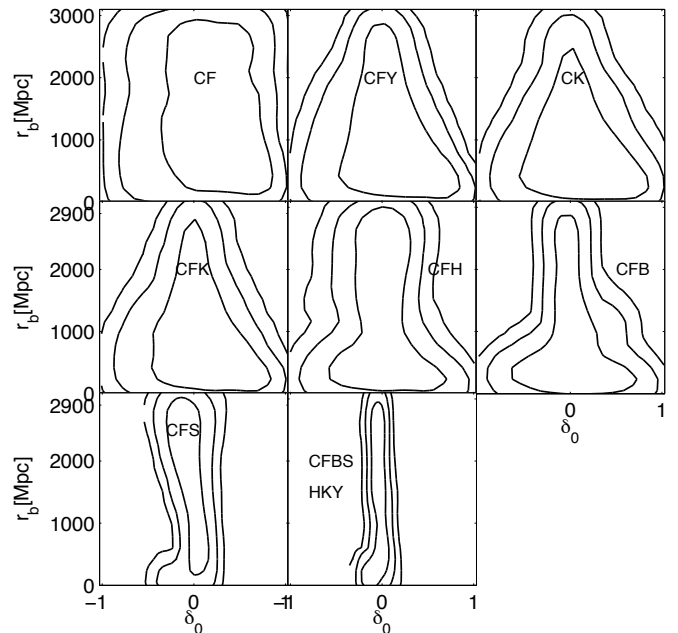


Figure 1. Marginalised constraints on r_b and δ_0 from different combinations of data, C refers to CMB, F to H_0 , B to BAO, S to SN, H to age data $H(z)$, K to kSZ, Y to Compton- y distortion. The constraints are ordered from left to right and top to bottom, by the allowed area. Naturally all datasets combined give the strongest constraints. See Fig. 2 for a comparison of the CFBSHKY plot to the Copernican prior.

Age data: Finally, we constrain radial inhomogeneity also by means of galaxy ages [25] using the maximum stellar age data from [26–28].

Copernican prior Given a gaussian density field, the root mean square of density perturbations inside a sphere of radius L around any point (hence also around the observer) today is

$$\sigma_L = \left[\int_0^\infty dk \frac{k^2}{2\pi^2} P(k) \left(\frac{3j_1(Lk)}{Lk} \right)^2 \right]^{\frac{1}{2}}, \quad (14)$$

where $P(k)$ is the matter power spectrum today inferred from the CMB temperature spectrum, assuming a Copernican universe, as a function of wavenumber k , and j_l is the spherical Bessel function of the first kind [29]. We calculate σ_L for the radius L at which the central over/under-density makes the transition to the surrounding mass-compensating under/over-dense shell. This transition occurs at a radius L slightly smaller than r_b . Then we compare the actual density perturbation of a certain inhomogeneity $\delta_0 \equiv M(r < L)/\bar{M} - 1$ and define the probability as $P(\delta_0, L) \propto \exp[-\frac{1}{2}(\delta_0/\sigma_L)^2]$. Note that we use the same normalization for different L so that the probability of having $\delta_0 = 0$ is the same.

Results We present our results in terms of the non-Copernican parameters δ_0 and r_b , marginalising over all

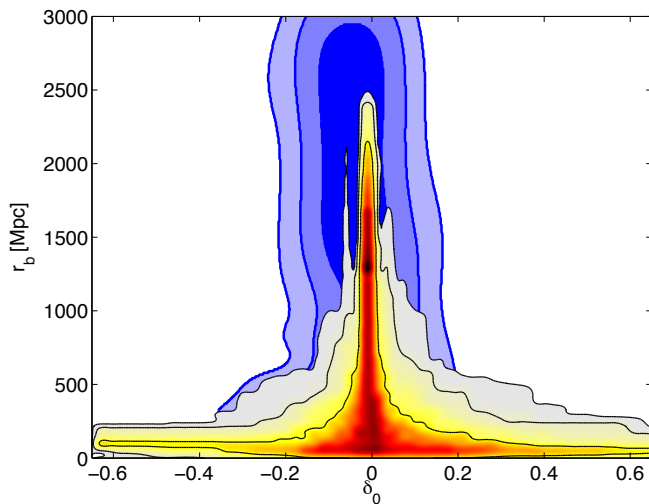


Figure 2. Marginalised posterior probability of r_b and δ_0 from all data sets combined (blue contours) at 68%, 95% and 99% confidence level (c.l.), compared to the Copernican prior obtained by fitting CMB only, (red to gray coloring) at 68%, 95% and 99% c.l. The ratio of the 99%-c.l. surfaces is roughly a factor of 3. Constraints on r_b and δ_0 need to improve by a factor of 3 to confirm the Copernican principle.

other aforementioned parameters. It should be clear that for a Copernican universe we have $\delta_0 = 0$. In Fig. 1 we show the constraints on the non-Copernican parameters from a number of possible combinations of datasets, ordered by constraining power. In all cases we use the CMB and H_0 constrains in combination with at least one other dataset. In this combination it turns out the SNe are most constraining. Not surprisingly, all datasets combined provide the strongest constraints, only allowing for a narrow range of density contrasts, however for many radii. Clearly, when $\delta_0 \rightarrow 0$, constraints on the radius allow for $r_b \rightarrow \infty$.

The key result of this paper is shown in Fig. 2, where we compare the constraints from all datasets to the constraints from purely the Copernican prior. We find that constraints on r_b and δ_0 need to improve by a factor of 3 to confirm the Copernican principle, because then observations on the lightcone constrain inhomogeneity to within the range allowed for by the CMB power spectrum.

Finally, in Fig. 3 we show for the first time constraints on the cosmological constant, Λ , marginalized over the effect of inhomogeneities around us, compared to the same constraints without taking into account inhomogeneity. We find that error bars increase by 25% if one marginalizes over inhomogeneity.

Our constraints depend on a variety of assumptions, in particular that dark energy is described by a cosmological constant [10, 30] and that general relativity is the correct theory of gravity. Our constraints apply to inho-

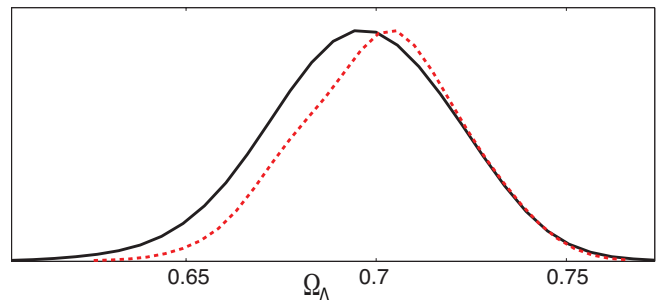


Figure 3. Marginalized posterior probability of the relative amount of dark energy (Ω_Λ) in the universe, when ignoring inhomogeneity (red dashed line), $\Omega_\Lambda = 0.70 \pm 0.04$ at 95% c.l., and when including inhomogeneity and marginalizing over it (solid black line), $\Omega_\Lambda = 0.69 \pm 0.05$ at 95% c.l. Both constraints come from CMB, H_0 , BAO, SN, $H(z)$, kSZ and Compton-y.

mogeneity which arises at late times, and do not apply to possible non-Copernican properties at early times. It is an important area for future study to generalise our results to these important cases.

-
- [1] V. Marra and A. Notari, *Class.Quant.Grav.* **28**, 164004 (2011), arXiv:1102.1015 [astro-ph.CO].
 - [2] C. Clarkson, *Comptes Rendus Physique* **13**, 682 (2012), arXiv:1204.5505 [astro-ph.CO].
 - [3] M. Scrimgeour, T. Davis, C. Blake, J. B. James, G. Poole, *et al.*, *Mon.Not.Roy.Astron.Soc.* **425**, 116 (2012), arXiv:1205.6812 [astro-ph.CO].
 - [4] J. Jackson, (2012), arXiv:1207.0697 [astro-ph.CO].
 - [5] B. Sinclair, T. M. Davis, and T. Haugbolle, *Astrophys. J.* **718**, 1445 (2010), arXiv:1006.0911 [astro-ph.CO].
 - [6] V. Marra and M. Paakkonen, *JCAP* **1012**, 021 (2010), arXiv:1009.4193 [astro-ph.CO].
 - [7] W. Valkenburg, *Gen.Rel.Grav.* **44**, 2449 (2012), arXiv:1104.1082 [gr-qc].
 - [8] J. Silk, *A&A* **59**, 53 (1977).
 - [9] J. P. Zibin, *Phys. Rev.* **D78**, 043504 (2008), arXiv:0804.1787 [astro-ph].
 - [10] V. Marra, M. Paakkonen, and W. Valkenburg, (2012), arXiv:1203.2180 [astro-ph.CO].
 - [11] W. Freedman *et al.* (HST Collaboration), *Astrophys.J.* **553**, 47 (2001), arXiv:astro-ph/0012376 [astro-ph].
 - [12] J. Guy, M. Sullivan, A. Conley, N. Regnault, P. Astier, *et al.*, *Astron.Astrophys.* **523**, A7 (2010), arXiv:1010.4743 [astro-ph.CO].
 - [13] A. Moss, J. P. Zibin, and D. Scott, *Phys.Rev.* **D83**, 103515 (2011), arXiv:1007.3725 [astro-ph.CO].
 - [14] T. Biswas, A. Notari, and W. Valkenburg, *JCAP* **1011**, 030 (2010), arXiv:1007.3065 [astro-ph.CO].
 - [15] E. Komatsu *et al.* (WMAP), *Astrophys. J. Suppl.* **192**, 18 (2011), arXiv:1001.4538 [astro-ph.CO].
 - [16] W. J. Percival *et al.* (SDSS Collaboration), *Mon.Not.Roy.Astron.Soc.* **401**, 2148 (2010),

- arXiv:0907.1660 [astro-ph.CO].
- [17] F. Beutler, C. Blake, M. Colless, D. H. Jones, L. Staveley-Smith, *et al.*, *Mon.Not.Roy.Astron.Soc.* **416**, 3017 (2011), arXiv:1106.3366 [astro-ph.CO].
- [18] C. Blake, E. Kazin, F. Beutler, T. Davis, D. Parkinson, *et al.*, *Mon.Not.Roy.Astron.Soc.* **418**, 1707 (2011), arXiv:1108.2635 [astro-ph.CO].
- [19] M. Zumalacarregui, J. Garcia-Bellido, and P. Ruiz-Lapuente, (2012), arXiv:1201.2790 [astro-ph.CO].
- [20] D. J. Fixsen *et al.*, *Astrophys. J.* **473**, 576 (1996), arXiv:astro-ph/9605054.
- [21] J. Garcia-Bellido and T. Haugboelle, *JCAP* **0809**, 016 (2008), arXiv:0807.1326 [astro-ph].
- [22] P. Zhang and A. Stebbins, *Phys.Rev.Lett.* **107**, 041301 (2011), arXiv:1009.3967 [astro-ph.CO].
- [23] J. P. Zibin and A. Moss, *Class. Quant. Grav.* **28**, 164005 (2011), arXiv:1105.0909 [astro-ph.CO].
- [24] E. Shirokoff, C. Reichardt, L. Shaw, M. Millea, P. Ade, *et al.*, *Astrophys.J.* **736**, 61 (2011), arXiv:1012.4788 [astro-ph.CO].
- [25] K. Bolejko, C. Hellaby, and A. H. A. Alfedeel, *JCAP* **1109**, 011 (2011), arXiv:1102.3370 [astro-ph.CO].
- [26] P. J. McCarthy *et al.*, *Astrophys. J.* **614**, L9 (2004), arXiv:astro-ph/0408367.
- [27] J. Simon, L. Verde, and R. Jimenez, *Phys. Rev.* **D71**, 123001 (2005), arXiv:astro-ph/0412269.
- [28] D. Stern, R. Jimenez, L. Verde, M. Kamionkowski, and S. A. Stanford, *JCAP* **1002**, 008 (2010), arXiv:0907.3149 [astro-ph.CO].
- [29] J. P. Henry, A. E. Evrard, H. Hoekstra, A. Babul, and A. Mahdavi, *Astrophys.J.* **691**, 1307 (2009), arXiv:0809.3832 [astro-ph].
- [30] I. Ben-Dayan, M. Gasperini, G. Marozzi, F. Nugier, and G. Veneziano, (2012), arXiv:1207.1286 [astro-ph.CO].